

**AN “ION SWITCH” REGULATES FUSION OF CHARGED MEMBRANES**

Evgenios Siepi<sup>\*</sup>, Silke Lutz<sup>\*</sup>, Sylke Meyer<sup>†</sup>  
and Steffen Panzner<sup>\*,†</sup>

<sup>\*</sup>Novosom AG , Weinbergweg 23, 06120 Halle, Germany

<sup>†</sup>Fraunhofer Center für Silizium-Photovoltaik, Walter-Hülse-Straße 1, 06120 Halle, Germany

<sup>‡</sup>corresponding author, email to [steffen.panzner@novosom.com](mailto:steffen.panzner@novosom.com)

Keywords:

liposomes – fusion - solvent ions – amphoteric liposomes – lipid shape theory

**Abstract**

We here identify the recruitment of solvent ions to lipid membranes as the dominant regulator of the lipid phase behavior. Our data demonstrate that binding of counterions to charged lipids promotes the formation of lamellar membranes, whereas their absence can induce fusion. The mechanism applies to anionic, cationic or the recently introduced amphoteric liposomes. In the latter, an additional pH-dependent lipid salt formation between anionic and cationic lipids must occur as indicated by the depletion of membrane-bound ions in a zone around p*H*5. Amphoteric liposomes fuse under these conditions, but form lamellar structures both at lower and higher p*H*.

The integration of these observations into the classic lipid shape theory yielded a quantitative link between lipid and solvent composition and the physical state of the lipid assembly. The key parameter of the new model,  $\kappa(\text{pH})$ , describes the membrane phase behavior of charged membranes in response to their ion loading in a quantitative way.

**Introduction**

Liposomes have recently re-gained much attention as carriers for oligonucleotides (ONs) such as antisense deoxynucleotides or siRNA. To be active, these large and highly charged molecules must be imported into the cytosol or the nucleus, a process that can be facilitated by liposomes.(4, 28) A fundamental problem during this import lies in the transition between a cargo retaining state of the carrier outside the cell and the release of the encapsulated substance upon cellular contact. The low p*H* found in endosomes provides a trigger for such transformation and acid-induced fusion has been observed for lipid materials such as cholesterol hemisuccinate (CHEMS) or phosphatidylserine, where the carboxyl function serves as the p*H* sensor.(8, 10, 15) A major practical limitation of these anionic liposomes, however, is their limited ability to encapsulate ONs due to a lack of electrostatic interaction.(6, 13) Cationic liposomes, on the other hand, effectively sequester ONs, but display unspecific binding to serum components or endothelia.(24-26) We recently demonstrated that both efficient loading of ON and high biocompatibility can be achieved using amphoteric liposomes.(1) These carriers adopt a cationic state at low p*H*, but have anionic character at neutral p*H*. When investigating the p*H*-dependent fusion of amphoteric liposomes, we noticed the unexpected coexistence of two stable, lamellar phases that are observed at both low and neutral p*H* with a fusogenic state that is limited to a zone around the isoelectric point of these membranes, typically about p*H* 5. This observation stands in contrast to findings reported elsewhere describing a single, continuous transition between the lamellar and hexagonal phase of amphoteric membranes; a discrepancy that prompted us to investigate the fusion mechanism of amphoteric liposomes.(7, 17) For that, we first re-examined the phase behavior of the individual anionic or cationic species before analyzing the more complex amphoteric assemblies.

### ***Materials and Methods***

The syntheses of MoChol and CHIM are described in (1) and (2), respectively.

Lipid structures, partial molecular volumes and pK (table 1) Lipids, their abbreviations, structural formula, partial molecular volumes and ionization constants are listed in table 2. Calculated pK were obtained using the pK module of the ACD/Labs 7.0 (Advanced Chemistry Development Inc., Toronto, Canada) and further adjusted by +1 or -0.5 for lipid anions or cations, respectively to reflect the deviations between calculated and experimentally determined pK. For calculation purposes only, the pK of the ammonium group was set as 15 to merely reflect the constant charge of this moiety. Values with an underscore were used for the calculations.

All molecular volumes were determined using DS Viewer Pro5.0 (Accelrys Software Inc., San Diego, CA). For cholesterol, the coordinate file CLR of the Protein Data Bank, <http://www.rcsb.org/pdb>, was used to ensure the proper conformation of the molecule. The split point between the apolar and polar portion of each molecule was defined as the 3' carbon/oxygen bond for cholesterol derivatives or as the C2-C3 bond for all diacylglycerols.

### Molecular volumes for hydrated ions (table 2)

The radii of the hydrated alkali ions were taken from (20) and first converted into their space filling molecular volumes  $v_{sp}$ . The hydration number  $n_H$  for these ions was then calculated using the space filling volume for water of 29,9 Å<sup>3</sup> (19). Further hydration numbers for acetate and chloride were obtained from (21); for dihydrogenphosphate  $n_H=9$  is used as supported by (21, 27). Hydration numbers for the amino acids were obtained as the combined values of their side chains as reported in (14) and of their zwitterionic portion (16, 23). For imidazole and tris-(hydroxymethyl)aminomethane, the hydration numbers of the histidine and lysine side chains were used, respectively. The volumes for the central ions devoid of their coordinated waters were obtained from (20) in case of the alkali ions and chloride, the van der Waals volumes for all other ions or water were determined using the DS viewer Pro5.0 software.

The volumes of the hydrated ions  $v_{HI}$  were then calculated as  $v_x + n_H \cdot v_{H_2O}$ , wherein  $v_x$  is the crystal volume of the alkali ion and  $v_{H_2O}$  is the volume of a water molecule.

Fusion after counterion discharge: Dowex® 50WX2 was freshly prepared in its hydrogen form using 1N hydrochloric acid; Dowex® 1X2 was converted into its OH<sup>-</sup> form using 1N sodium hydroxide and both materials were extensively rinsed with water. FRET labeled liposomes were produced by injecting 320 µl of the 20mM lipids in isopropanol into 10ml of 50mM acetic acid, 50mM imidazole, pH 6. Both labeled species were combined and portions of the ion exchange materials were added. Aliquots were taken at pH 5, 4 and 3 upon addition of Dowex 50WX2 or at pH 7 or 8 upon addition of Dowex 1X2. Liposomes were incubated for 2h at 37°C after which the pH was adjusted back to 6 using acetic acid or imidazole and FRET signals were measured.

pH dependent fusion of CHEMS and CHIM: CHEMS was dissolved in isopropanol at a concentration of 20mM and supplied with 1mol% NBD-PE or N-Rh-PE, respectively and liposomes were formed by injecting 100µl of the lipid solution into 700µl of buffer A (10mM acetic acid and phosphoric acid, pH 7.5 adjusted with NaOH). 100µl of NBD-PE-labelled and 100µl N-Rh-PE-labelled liposomes were mixed together with 200µl buffer A. Aliquots of 50µl were brought to the indicated pH using 50µl of 5x buffer A adjusted to the target pH values. Fusion was allowed for 2h at 37°C after which the suspensions were neutralized to pH 7.5 using 50µl of appropriately concentrated NaOH to more clearly distinguish between liposome aggregation and fusion. Fluorescence was recorded after completion of the pH

cycle. Liposomes from CHIM were produced from 20mM CHIM in isopropanol as above and fusion of CHIM in the presence of chloride ions was investigated in buffers comprising 10mM of L-lysine, pyridine and imidazole which were adjusted to the respective pH values with hydrochloric acid. Individually labeled liposomes from CHIM were produced at pH 4 and brought to the indicated pH using 5x buffer. Fusion was allowed for 2h and fluorescence was recorded after re-adjustment to pH 3.8.

Fusion of amphoteric liposomes in response to pH: Liposomes were prepared by injecting lipid mixtures in isopropanol (20mM) in buffer A to a final concentration of 3mM. 100µl of NBD-PE-labelled and 100µl N-Rh-PE-labelled liposomes of otherwise identical composition were mixed together with 200µl buffer A. Aliquots of 50µl were adjusted to the indicated pH using 50µl of 5x buffer A adjusted to the respective pH. Fusion was allowed for 2h at 37°C after which FRET signals were recorded. To discriminate between fusion and mere aggregation, the suspensions were then neutralized to pH 7.5 using 50µl of appropriately concentrated NaOH and fluorescence was recorded again. All liquid handling was performed using a Multiprobe II Ex robot (Perkin Elmer, Waltham, MA) in black 96 well plates. The presence of residual amounts of isopropanol did not result in any appreciable change of the fusion properties.

Ion binding: 300µl of 30mM lipid solutions in isopropanol were injected into 2ml of 10mM sodium phosphate, pH 7.5. Liposomes were separated from solvent ions using PD10 columns (GE, Uppsala, Sweden) equilibrated in 15% isopropanol/water. Lipid recovery was about 80%. Liposome bound sodium and phosphorus concentrations were determined using an Element 2 Inductively Coupled Plasma Mass Spectrometer (Thermo Scientific, Bremen, Germany) as described in (5).

Further Materials and Methods as well as mathematical considerations are described in the Supporting Materials.

## Results

### *Membrane fusion is regulated by counterion binding*

The stabilization of pH-sensitive bilayers, e.g. from CHEMS, has been explained by the hydration of the charged head group, the electrostatic repulsion between these moieties, through binding of counterions or a combination of these elements.(8, 17) To discriminate between these assumptions we analyzed the fusion of charged and uncharged bilayers of CHEMS under conditions of counterion binding or dissociation. Fusion was monitored through lipid mixing between individually labeled membranes using fluorescence resonance energy transfer (FRET). For that, particles were prepared and mixed at neutral pH, incubated at various lower values of pH, and eventually neutralized to discriminate fusion from mere agglomeration.

Liposomes from anionic CHEMS (pK~5.4, table 1) were prepared at pH 6 in the presence of charged imidazolium ions (pK=7,0 in (3)). The lipid particles were stable and did not fuse as commonly expected by the theories mentioned above.

We then discharged the imidazolium ions by adding small portions of the anion exchange resin DOWEX®1X2 in its OH<sup>-</sup> form; a technique that liberates hydroxyl ions and raises the pH, but avoids the addition of interfering cations. The procedure resulted in fusion of CHEMS membranes at neutral or alkaline pH. If the pH of the CHEMS:imidazol system was raised through the addition of sodium hydroxide, no fusion was observed.(fig. 1A,B) This difference in the experimental outcome de-emphasizes electrostatic repulsion or head group hydration as mechanisms stabilizing the lamellar phase, as these relate to the charge status of CHEMS, a variable that is unchanged in the experiment. Instead, our data identify ion decoration as a critical component. Consistent with that, protonation of CHEMS at low pH resulted in fusion regardless whether this was achieved through addition of hydrochloric acid or by using H<sup>+</sup> loaded ion exchange materials. In both cases, CHEMS loses its ion binding capacity through protonation of its polar headgroup.

Liposomes made from a cationic, pH sensitive cholesterylimidazol (CHIM (2), pK~6.4) showed a reciprocal behavior. Fusion was not observed between membranes of CHIM in the presence of acetate ions at pH 6, but was induced upon addition of the cation exchanger DOWEX®50WX2 in its H<sup>+</sup> form. As protons are released from the cation exchanger, acetate ions are neutralized; a change which in turn can lead to their dissociation from the membrane. In contrast, no phase transition was achieved upon direct acidification with hydrochloric acid. Since CHIM is positively charged regardless of the way acidification of the medium is achieved, the difference in its phase behavior most likely relates to the recruitment of the counterions from solvent. The chloride ions introduced with HCl apparently bind to the imidazole head groups of CHIM, thereby stabilizing the lamellar state of the membrane, whereas acidification using DOWEX50WX2 does not introduce the stabilizing chloride ions and fusion is observed. Fusion of CHIM liposomes at higher pH was observed both upon addition of OH<sup>-</sup> loaded ion exchange materials, but also upon adjustment of the pH with sodium hydroxide (fig. 1C,D). In both cases, CHIM loses its cationic charge and therefore its ability to bind solvent ions. As with CHEMS, fusion of CHIM coincides with ion recruitment to the bilayer, but is not linked to head group repulsion or hydration.

***Ion size inversely relates to fusion***

Since ion binding coincides with the appearance of a non-fusogenic state of the membrane, we were interested whether the size of the bound ions can modulate fusion. To test this, we prepared FRET labeled liposomes from CHEMS and cholesterol (15:85 mol%) and monitored lipid mixing over time. Decreased lipid mixing was observed in the series of  $K^+ > Na^+ > Li^+ > \text{tris(hydroxymethylaminomethan)}^+ > \text{arginine}^+$ . Control reactions using anions of different size in combination with  $Na^+$  did not result in notable differences of the fusion process (fig. 2A). Conversely, the fusion of cationic liposomes made from CHIM: cholesterol (20:80 mol%) was enhanced in the order of  $Cl^- > \text{acetate}^- > \text{glutamate}^-$ , but was unchanged in acetate buffers comprising  $K^+$ ,  $Na^+$  or  $Li^+$  cations (fig. 2B).

The fusogenicity of a charged membrane therefore depends on the size of the attracted ions and large counterions interfere more strongly with membrane fusion than smaller ones. The ions in water exist as hydrated species, a fact that we took into account for their molecular volumes in table 2.

Taken together, our results support an “ion switch” model for membrane fusion. In this model, the presence of lipid-bound solvent ions promotes membrane stability while their absence can lead to fusion.

***Amphoteric liposomes show a double phase transition***

Mixtures of anionic and cationic lipids can form amphoteric liposomes, provided that at least one of the components is pH-sensitive. From our analysis above amphoteric membranes were expected to have little or no phase transition, since the membrane stabilizing ion binding of the anionic lipid would complement that of the cationic amphiphile. Alternatively, amphoteric liposomes formed from a constantly charged cationic lipid in combination with CHEMS should display a dampened, but continuous phase transition, as described by Hafez.(7) In contrast to this earlier report, we observed lipid fusion at pH 6 and pH4.5, but the existence of lamellar structures both at pH 7.5 and pH 3 for amphoteric liposomes from CHEMS and dioleoyl-(trimethylammonium)propanediol, (DOTAP, fig. 3).

This observation prompted us to systematically probe the pH-induced fusion for binary mixtures of CHEMS and DOTAP. For amphoteric systems, that is mixtures having an excess of CHEMS, reduced lipid mixing and maintenance of particle size was observed at both neutral and low pH, but fusion occurred around pH 5. This double phase transition is unique to amphoteric mixtures and was not observed in cationic blends having an excess of DOTAP (fig. 4A,B). Vesicles rich in DOTAP display a size increment but do not fuse. We attribute this to a crosslinking of DOTAP liposomes in the presence of the bivalent phosphate ions since the effect disappeared in the presence of monovalent buffers.

Following the initial expectation and given the non-fusogenic character of DOTAP (18), the addition of it should have dampened the acid-induced fusion of CHEMS. Instead, we observed fusion at slightly acidic conditions and the existence of two lamellar phases at both neutral and acidic pH in amphoteric mixtures of the oppositely charged lipids. We explain this with the formation of an intrabilayer lipid salt; a structure that is fusion promoting as its devoid of solvent counterions.



***DOTAP and CHEMS form a lipid salt devoid of counterions***

To test the occupancy of mixtures from DOTAP and CHEMS with solvent ions we generated liposomes in sodium phosphate buffer at pH 7.5 and separated unbound ions by gel filtration in pure water. Lipid bound sodium or phosphorus were then quantified by inductively coupled plasma mass spectroscopy (ICP-MS). Apart from low amounts of passively trapped sodium or phosphate, we measured low levels of bound solvent ions in samples having nearly equal amounts of DOTAP and CHEMS.(fig.5) Liposomes having an excess of CHEMS did adsorb sodium, but only background levels of phosphorus whereas those having an excess of DOTAP recruited phosphate almost exclusively. Eventually, the adsorbed amounts were in proportion to the excess of the respective lipid, not to its total amount. Taken together these facts support the formation of an ion-free lipid salt within mixed bilayers of DOTAP and CHEMS. For the remainder of free, unpartnered lipid our data provide direct experimental evidence for a recruitment of solvent ions to charged lipid species.

***Quantitative modeling***

We next set out to quantify our observations using the framework of the lipid shape theory; a model which relates membrane fusion to a low aspect ratio between the polar and apolar region of a lipid and formation of a lamellar phase to higher such ratios.(11) The important role of ions in membrane fusion and stabilization required an extension of the classic model. We here include ions as volume contributing elements of the lipid structures. In the example, binding of a hydrated sodium ion adds 93 Å<sup>3</sup> to the volume of the hemisuccinate portion of CHEMS that by itself occupies only 78 Å<sup>3</sup>. Conversely, a hydrated dihydrogenphosphate ion adds 176 Å<sup>3</sup>, respectively, to the head group of DOTAP, which itself has only a volume of only 57 Å<sup>3</sup>. The volume contribution made by a bound ion is therefore substantial.

The general function for the pH-dependent phase behavior of a charged bilayer can now be written as:

$$(1) \kappa(\text{pH}) = (x \cdot V_{\text{AH}} + (1-x) \cdot V_{\text{CH}} + x_{\text{I}} \cdot V_{\text{I}}) / (x \cdot V_{\text{AT}} + (1-x) \cdot V_{\text{CT}}),$$

wherein  $\kappa$  describes the volume ratio between all polar and apolar elements of the bilayer and  $x$  the molar fraction of the anionic lipid. The polar elements comprise the head group volumes  $V_{\text{AH}}$  and  $V_{\text{CH}}$  of the lipid anion and cation and an amount  $x_{\text{I}}$  of the respective counterions having a volume  $V_{\text{I}}$ , the latter being equal to the fraction of charged, but unpaired lipid head groups  $x_{\text{I}} = |x_{\text{A}^-} - x_{\text{C}^+}| = x / (1 + c_{\text{H}^+} / K_{\text{A}}) - (1-x) / (1 + K_{\text{C}} / c_{\text{H}^+})$  wherein  $K_{\text{A}}$  and  $K_{\text{C}}$  are the respective ionization constants of the lipid anion and cation and  $c_{\text{H}^+}$  is the proton concentration. The apolar volume elements are contributed by the tail volumes  $V_{\text{AT}}$  and  $V_{\text{CT}}$ , respectively.

For membranes comprising both anionic and cationic lipids  $\kappa(\text{pH})$  describes the stabilization of a lipid membrane through attraction of a counterion volume  $V_{\text{I}}$  to the portion  $x_{\text{I}}$  of charged lipid molecules that do not form the lipid salt. Low values for  $\kappa$  indicate the fusogenic state of the lipid assembly which relates to a relatively small head group volume whereas higher values are linked to the formation of a lamellar phase. When calculated for amphoteric mixtures of CHEMS and DOTAP,  $\kappa(\text{pH})$  reflects the stable lipid phases observed at both low and high pH. Secondly, a fusogenic phase around the isoelectric point appears both in the experiment and in  $\kappa(\text{pH})$ . Thirdly,  $\kappa(\text{pH})$  follows the single-sided, monophasic pH-dependency for CHEMS. Fourthly, the calculation predicts the non-fusogenic bilayers observed for mixtures having an excess of DOTAP or being formed from pure DOTAP and fifthly, low values for  $\kappa(\text{pH})$  predict a fusogenic state for the equimolar mixture of DOTAP and CHEMS (fig. 6). In fact, we observed lipid mixing for this composition at neutral pH.

***Biphasic stability is a general feature of amphoteric liposomes***

Expanding on these results, we also analyzed amphoteric liposomes in which both the anionic and cationic lipid are pH sensitive. These systems are classified here as “amphoter II” in contrast to the “amphoter I” comprising a weak anionic amphiphile in combination with a strong lipid cation.

Indeed, amphoter II liposomes constructed from either CHIM:CHEMS or analogous systems composed of the morpholinocholesterol MoChol (1) and CHEMS do also show biphasic stability and fusion around their respective isoelectric points (fig. 7A, B). If MoChol is used as the cationic component, this behavior was limited to mixtures having an excess of CHEMS, whereas composition rich in MoChol do no longer undergo pH-induced fusion. We attribute this to the rather large polar head group of MoChol which does suppress fusion by contributing volume to this portion of the molecule; quite analogously to the binding of very large counterions. Calculations according to eq. (1) reflect the lipid phase behavior of both amphoter II systems in detail; low values for  $\kappa(\text{pH})$  coincide with the occurrence of lipid mixing whereas higher values for  $\kappa(\text{pH})$  indicate the formation of a lamellar phase (fig. 8 A,B).

Biphasic stability was also observed for an amphoter III system comprising the stably charged anionic lipid dioleoylphosphatidic acid (DOPA) and an excess of the pH-dependent cationic lipid MoChol and is reflected in the respective function  $\kappa(\text{pH})$  as shown in figure 9. For these calculations the monovalent form of DOPA was used as this is the prevalent form of the molecule below pH7, a condition that is required for the protonation of MoChol. One should, however, keep in mind that DOPA acquires an additional charge above pH7 and possibly binds a second counterion which may lead to a further increase of its head group size. An interesting exemption from the general picture presented here is the absence of fusion in MoChol:POPG which may be caused by steric hindrance. (Fig S2 in the Supporting Materials)

***Discussion***

This work features lipid bound ions as a regulator of membrane fusogenicity, a model in which ion adsorption stabilizes charged membranes, whereas ion desorption can lead to fusion. This was directly demonstrated using the novel approach of counterion discharge, which enables the preparation of charged, but ion depleted lipid membranes. Charged membranes in the presence of discharged counterions undergo fusion as evidenced by lipid mixing from differently labeled membranes. Since the charge of the polar lipid head group remains constant during the counterion discharge, the observed phase transition cannot be explained by changes in the electrostatic repulsion between individual lipids or variations of lipid headgroup hydration. The fusogenicity of these systems was even sufficient to overcome the electrostatic repulsion between lipid particles. Altogether, this leaves the counterion binding as the most direct explanation for the experimental observations and the reduced membrane fusion in the presence of larger counterions suggests that the volume rather than the chemistry of an ion is important. Ion recruitment to charged bilayers is sufficient to explain the well described fusion of CHEMS-liposomes upon acidification (8), it also reflects the fusion of CHIM-liposomes at higher pH. (fig. S1 and S3 of the Supporting Materials) Recent molecular dynamics simulations confirm the recruitment of solvent ions to bilayers of CHEMS in response to the charge of the lipid.(12)

The pH related stabilization of charged lipid membranes occurs in a reciprocal fashion for anionic or cationic lipids. Mixed membranes were therefore expected to be stable over the entire range of pH conditions. This is clearly not the case as demonstrated for various amphoteric liposomes constructed from weak lipid anions and strong cations (amphoter I), weak lipid anions and weak cationic amphiphiles (amphoter II) or for mixtures of strong lipid anions and weak cationic amphiphiles (amphoter III), respectively. Instead, most of these



systems undergo fusion around their isoelectric point. We explain this by the formation of a lipid salt whereby the two oppositely charged amphiphiles neutralize each other. Lipid salt formation leads to a displacement of counterions and a concomitant reduction in the head group volume which in turn causes fusion. Experimental evidence for the hypothesized lipid salt formation is provided through quantitative analysis of the membrane bound solvent ions in binary mixtures of DOTAP and CHEMS which shows minimized ion decoration under conditions of charge neutralization. In addition, we observed ion selectivity for mixtures having a modest excess of CHEMS or DOTAP; a fact that is best explained by the sequestration of the minor lipid component in a lipid salt, so that only the lipid in excess is available for counterion recruitment and membrane stabilization. In systems having an overage of CHEMS, sodium recruitment is sufficient to stabilize the lamellar phase of the DOTAP: CHEMS membrane at neutral pH. Acidification reduces the amount of charged CHEMS in the system until - at the isoelectric point - its molar fraction is equal to that of DOTAP. The membrane is now ion-free and highly fusogenic, as all charged CHEMS forms a lipid salt with DOTAP while the remainder of the anionic lipid is protonated. Further acidification produces more uncharged CHEMS, which leads to a liberation of DOTAP from the lipid salt, recruitment of acetate or phosphate and concomitant membrane stabilization. (fig. S3 of the Supporting Materials)

Taken together, the binding of solvent ions to charged lipid headgroups is a dominant regulator of the phase behavior of lipid membranes. The process provides a universal explanation for the seemingly different fusion processes observed in charged, but ion-depleted systems or discharged membranes; in combination with the formation of a lipid salt it also fully explains the complex phase behavior of amphoteric membranes.

The important role of lipid bound ions created a need to extend the classic lipid shape theory which relates lipid geometry to phase behavior. We now introduce the lipid bound ion as an integral component of the lipid head group, contributing to its volume. This novel, “dynamic shape theory” reflects the pH-dependent ion recruitment to lipid bilayers and describes the lipid phase behavior in context with a solvent. Our model calculations reflect the complex phase behavior observed in the experiments and yield quantitative results within a given system or for related systems. We noticed though that the fusion of DOTAP: CHEMS starts at lower values of  $\kappa$  compared to that of amphoteric II or III systems. One may relate this to the nature of the hydrophobic tail regions; however, both the amphoteric I and amphoteric III systems represent a combination of a diacylglycerol and a sterol, while the amphoteric II systems are entirely sterol based. Thus, the split point between the apolar and polar lipid fragments remains a sensitive variable in any lipid shape calculations.

A second variable is the actual volume contribution of the counterions, as these exist as hydrated species in water and their hydration numbers  $n_H$  may vary with the method of their determination (21) or during salt formation or complexation.(22) In our calculations, we consider  $n_H$  of a charged lipid head group in complex with its counterion being equal to that of the hydrated solvent ion; an assumption that can account for the partial reduction of the hydration shells of both the lipid and the solvent ion during complexation. The uncertainty related to  $n_H$ , however, is modest as  $\Delta n_H$  of 2 results in an inaccuracy of about 15% when calculated for sodium hemisuccinate. More importantly, assumptions for  $n_H$  never affect the qualitative outcome of the model, they only change the degree of stabilization achieved by ion binding.

Altogether, we here identify membrane bound ions or an “ion switch” as a key regulator of the stability of charged membranes. This initial discovery, together with the hypothesis of a lipid salt formation was then used to explain the double phase transitions of amphoteric liposomes. Eventually, our observations led to a “dynamic shape theory” which describes the membrane in its context with solvent ions. Our future work will demonstrate the applicability of this theory for multi-component systems involving neutral lipids and shall eventually

facilitate a rational prediction between liposome composition and performance in cell transfection.

### Acknowledgement

The authors gratefully acknowledge the technical help of Ute Vinzens and Claudia Müller. For the electron microscopy we thank Frank Steiniger, University of Jena.

### Author Contributions

ES established, performed and analyzed individual and high-throughput fusion assays. SL did conceptual and analysis works in the fusion experiments. SM and SP did the ICP-MS analysis and SP developed the concepts, the dynamic shape theory and wrote the manuscript.

### Competing Financial Interest

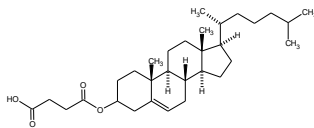
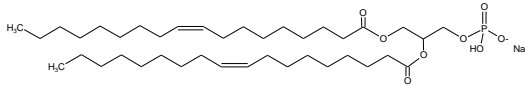
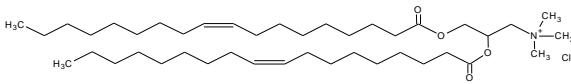
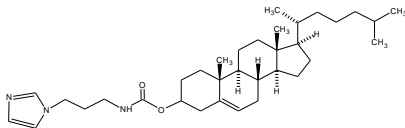
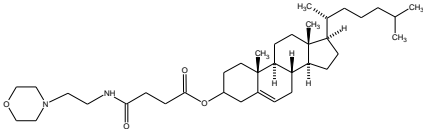
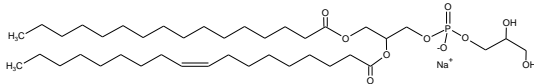
The authors declare no competing financial interest.

### Reference List

1. Andreakos, E., U. Rauchhaus, A. Stavropoulos, G. Endert, V. Wendisch, A. S. Benahmed, S. Giaglis, J. Karras, S. Lee, H. Gaus, C. F. Bennett, R. O. Williams, P. Sideras, and S. Panzner. 2009. Amphoteric liposomes enable systemic antigen-presenting cell-directed delivery of CD40 antisense and are therapeutically effective in experimental arthritis. *Arthritis Rheum.* 60: 994-1005.
2. Budker, V., V. Gurevich, J. E. Hagstrom, F. Bortzov, and J. A. Wolff. 1996. pH-sensitive, cationic liposomes: a new synthetic virus-like vector. *Nat. Biotechnol.* 14: 760-764.
3. Datta, S. P., and A. K. Grzybowski. 1966. The acid dissociation constant of the imidazolium ion. *J. Chem. Soc. B* : 136-140
4. de Fougerolles, A., H. P. Vornlocher, J. Maraganore, and J. Lieberman. 2007. Interfering with disease: a progress report on siRNA-based therapeutics. *Nat. Rev. Drug Discov.* 6: 443-453.
5. DIN 50451-4. 2007. Testing of materials for semiconductor technology - Determination of trace elements in liquids - Part 4: Determination of 34 elements in ultra pure water by mass spectrometry with inductively coupled plasma (ICP-MS). Beuth-Verlag, Berlin.
6. Foged, C., H. M. Nielsen, and S. Frokjaer. 2007. Liposomes for phospholipase A2 triggered siRNA release: preparation and in vitro test. *Int. J Pharm* 331: 160-166.
7. Hafez, I. M., S. Ansell, and P. R. Cullis. 2000. Tunable pH-sensitive liposomes composed of mixtures of cationic and anionic lipids. *Biophys. J.* 79: 1438-1446.
8. Hafez, I. M., and P. R. Cullis. 2000. Cholesteryl hemisuccinate exhibits pH sensitive polymorphic phase behavior. *Biochim. Biophys. Acta.* 1463: 107-114.
9. Heyes, J., L. Palmer, K. Bremner, and I. MacLachlan. 2005. Cationic lipid saturation influences intracellular delivery of encapsulated nucleic acids. *J Control Release* 107: 276-287
10. Hope, M. J., and P. R. Cullis. 1980. Effects of divalent cations and pH on phosphatidylserine model membranes: a <sup>31</sup>P NMR study. *Biochem. Biophys. Res. Commun.* 92: 846-852.
11. Israelachvili, J. N., D. J. Mitchell, and B. W. Ninham. 1977. Theory of self-assembly of lipid bilayers and vesicles. *Biochim. Biophys. Acta.* 470: 185-201.
12. Klasczyk, B., S. Panzner, R. Lipowsky, and V. Knecht. 2010. Fusion-relevant changes in lipid shape of hydrated cholesterol hemisuccinate induced by pH and counterion species. *J Phys Chem B* 114: 14941-14946.
13. Klimuk, S. K., S. C. Semple, P. N. Nahirney, M. C. Mullen, C. F. Bennett, P. Scherrer, and M. J. Hope. 2000. Enhanced Anti-Inflammatory Activity of a Liposomal Intercellular Adhesion Molecule-1 Antisense Oligodeoxynucleotide in an Acute Model of Contact Hypersensitivity. *J Pharmacol Exp Ther* 292: 480-488.
14. Kuntz, I. D., Jr., and W. Kauzmann. 1974. Hydration of proteins and polypeptides. *Adv. Protein Chem.* 28:239-345.: 239-345.

15. Lai, M. Z., W. J. Vail, and F. C. Szoka. 1985. Acid- and calcium-induced structural changes in phosphatidylethanolamine membranes stabilized by cholesteryl hemisuccinate. *Biochemistry*. 24: 1654-1661.
16. Leung, K., and S. B. Rempe. 2005. Ab initio molecular dynamics study of glycine intramolecular proton transfer in water. *J Chem Phys* 122: 184506.
17. Li, X., and M. Schick. 2001. Theory of tunable pH-sensitive vesicles of anionic and cationic lipids or anionic and neutral lipids. *Biophys. J.* 80: 1703-1711.
18. Loney, C., M. F. Lensink, E. Kleiren, J. M. Vanderwinden, J. M. Ruyschaert, and M. Vandenbranden. 2010. Fusogenic activity of cationic lipids and lipid shape distribution. *Cell Mol. Life Sci.* 67: 483-494.
19. Nagle, J. F., R. Zhang, S. Tristram-Nagle, W. Sun, H. I. Petrache, and R. M. Suter. 1996. X-ray structure determination of fully hydrated L alpha phase dipalmitoylphosphatidylcholine bilayers. *Biophys. J* 70: 1419-1431.
20. Nightingale, E. R. Jr. 1959. Phenomenological Theory of Ion Solvation. Effective Radii of Hydrated Ions. *J Phys Chem* 63: 1381-1387.
21. Ohtaki, H., and T. Radnai. 1993. Structure and Dynamics of Hydrated Ions. *Chem Rev* 93: 1157-1204.
22. Pandit, S. A., D. Bostick, and M. L. Berkowitz. 2003. Molecular dynamics simulation of a dipalmitoylphosphatidylcholine bilayer with NaCl. *Biophys. J.* 84: 3743-3750.
23. Parsons, M. T., and Y. Koga. 2005. Hydration number of glycine in aqueous solution: an experimental estimate. *J Chem Phys.* 123: 234504.
24. Reinsch, C., E. Siepi, A. Dieckmann, and S. Panzner. 2008. Strategies for the Delivery of Oligonucleotides in vivo. In *Therapeutic Oligonucleotides*. J. Kurreck, editor. Royal Society of Chemistry, Cambridge. 226-237.
25. Santel, A., M. Aleku, O. Keil, J. Endruschat, V. Esche, G. Fisch, S. Dames, K. Löffler, M. Fechtner, W. Arnold, K. Giese, A. Klippel, and J. Kaufmann. 2006. A novel siRNA-lipoplex technology for RNA interference in the mouse vascular endothelium. *Gene Ther.* 13: 1222-1234.
26. Semple, S. C., S. K. Klimuk, T. O. Harasym, S. N. Dos, S. M. Ansell, K. F. Wong, N. Maurer, H. Stark, P. R. Cullis, M. J. Hope, and P. Scherrer. 2001. Efficient encapsulation of antisense oligonucleotides in lipid vesicles using ionizable aminolipids: formation of novel small multilamellar vesicle structures. *Biochim. Biophys. Acta* 1510: 152-166.
27. Tang, E., T. D. Di, and N. H. de Leeuw. 2009. Hydrogen transfer and hydration properties of  $H(n)PO_4(3-n)$  ( $n=0-3$ ) in water studied by first principles molecular dynamics simulations. *J Chem Phys* 130: 234502.
28. Whitehead, K. A., R. Langer, and D. G. Anderson. 2009. Knocking down barriers: advances in siRNA delivery. *Nat. Rev. Drug Discov.* 8: 129-138.

TABLE 1 Description of lipids

Abbreviation and Name	Structure	Head vol [ $\text{\AA}^3$ ] Tail vol. [ $\text{\AA}^3$ ]	pK <sup>1</sup>
<b>CHEMS</b> Cholesteryl hemissuccinate		78.2 343	<u>5.41</u> 5.53 <sup>2</sup> 5.8 <sup>3</sup>
<b>DOPA</b> 1,2-Dioleoyl-sn-glycero-3-phosphate		62.8 511.8	7.38 <u>2.83</u>
<b>DOTAP</b> N-[1-(2,3-Dioleoyloxy)propyl]-N,N,N-trimethylammonium chloride		57.2 511.8	<u>15</u>
<b>CHIM</b> Cholesterol-(3-imidazol-1-yl propyl)-carbamate		119.2 343	<u>6.36</u> 6.0 <sup>4</sup>
<b>MoChol</b> ( $\alpha$ -(3'-O-cholesteryloxycarbonyl)- $\delta$ -(N-ethylmorpholine)-succinamide)		168.2 343	<u>6.51</u> 6.50 <sup>2</sup>
<b>POPG</b> 1-Palmitoyl-2-oleoyl-sn-glycero-phosphatidylglycerol		115.9 490.4	<u>1.39</u>

<sup>1</sup> for the calculation and adjustment of pK values see Materials and Methods, underlined values were used for the calculation of the phase diagrams

<sup>2</sup> experimentally determined for pure lipids according to (9)

<sup>3</sup> reported in (8) for CHEMS:POPC 1:1 mixtures

<sup>4</sup> reported in (2) for micellar solutions of CHIM

TABLE 2 Molecular volumes for hydrated ions

Ion	$r_x$	$r_h$	$v_x$	$v_x$ data	$v_{app}$	$n_H$	$n_H$ data	$v_{HI}$
$Li^+$	0,60	3,82	1	(20)	233	7,8	calc	111
$Na^+$	0,95	3,58	4	(20)	192	6,3	calc	93
$K^+$	1,33	3,31	10	(20)	152	4,8	calc	77
$Cl^-$	1,81	3,32	25	(20)	153	4,3	calc	86
$Ac^-$			40	calc		5	(21)	111
$H_2PO_4^-$			48	calc		9	(21, 27)	176
$Glu^-$			98	calc		12,5	(14, 23)	275
$Imid^+$			51	calc		4	(14)	108
$Tris^+$			93	calc		4	(14, 21)	150
$Arg^+$			131	calc		8	(14, 23)	245

The crystal and hydrated radii of the ions are  $r_x$  and  $r_h$ , respectively;  $v_x$  is the volume of the central ion. The data source for these values is given in the following column. The apparent molecular volume of the hydrated ion is  $v_{app}$ ;  $n_H$  is the hydration number as calculated from space filling volumes or according to data referred in the next column. Eventually, the molecular volumes  $v_{HI}$  of the hydrated ions are listed. All radii and volumes are in Å or Å<sup>3</sup>, respectively.  $Ac^-$  acetate,  $Glu^-$  glutamic acid,  $Imid^+$  imidazolium,  $Tris^+$  tris-(hydroxymethyl)aminomethanium,  $Arg^+$  argininium

**FIGURE 1** Counterion dependent membrane fusion. **(A)** FRET labeled liposomes from CHEMS were formed in imidazole:acetate buffer at pH 6 and the pH was adjusted by addition of ion exchange materials in their  $H^+$  or  $OH^-$  form. Fusion of the lipid materials is observed both at high and low pH. **(B)** Liposomes as in (A) were produced in the presence of  $Na^+$  and the pH was adjusted by addition of acid or base. Fusion at low pH occurs as in (A) but no fusion is observed at high pH. **(C)** FRET-labelled liposomes from CHIM were formed and ion exchange materials were added as in (A). Fusion of the liposomes is observed both at high and low pH. **(D)** Liposomes as in (C) were formed in lysine/morpholine/imidazole buffer at pH 4. Stronger fusion was observed at high pH when CHIM becomes discharged.

**FIGURE 2** Counterion size modulates lipid membrane fusion. FRET labeled liposomes from CHEMS/Chol (15:85, A) or CHIM/Chol (20:80, B) were formed at pH 6 in buffers containing the indicated ions and lipid mixing between vesicles was monitored over time. **(A)** The extent of fusion follows the volumes  $v_{HI}$  of the hydrated counteranions as listed in table 2, while various counteranions do not affect the fusion properties of CHEMS/Chol. **(B)** Conversely, the large anion glutamic acid (Glu), but not chloride does suppress fusion of CHIM/Chol; different counteranions had no impact on fusion.

**FIGURE 3** Amphoteric liposomes display bistable phase behavior. Liposomes from DOTAP and CHEMS (45:55) were produced at pH 7.5, exposed to the pH indicated and examined using cryo transmission electron microscopy. The material forms a lamellar phase both at pH 7.5 and pH 3, but undergoes a phase transition at pH 6 or pH4.5. Bars = 200nm

**FIGURE 4** pH-induced fusion of binary mixtures from DOTAP and CHEMS. Systematically varied blends of DOTAP and CHEMS were dissolved in isopropanol, split and labeled with FRET marker lipids. After formation of the individually labeled liposomes, matching samples were recombined and the materials were exposed to conditions of slightly acidic pH for 2h, then re-adjusted to neutrality and pH induced fusion was monitored by the appearance of the FRET signal **(A)** or through the formation of larger particles in **(B)**. The size increment in (B) is denotes the ratio of the particle sizes before and after the pH cycle.

**FIGURE 5** Ion adsorption to lipid membranes. Liposomes from various mixtures of DOTAP and CHEMS were produced in sodium phosphate buffer and separated from unbound solvent ions through size exclusion chromatography in water. Bound sodium and phosphorus were measured by ICP-MS. The mixed membranes from DOTAP and CHEMS bind sodium whenever CHEMS is present in excess, but phosphorus in cases of excessive DOTAP. Quantitatively, the ion binding capacity of these membranes follows the presence of free charged lipid, which is the material not participating in the lipid salt. The ion binding reaches a minimum for equimolar mixtures of DOTAP and CHEMS.

**FIGURE 6** Calculated phase diagram for DOTAP/CHEMS under the assumptions of counterion binding and the formation of the ion free lipid salt. The volume ratio  $\kappa$  assumes a pH dependent minimum in the amphoteric mixtures having more than 50% CHEMS the appearance of which correlates with the fusion zone observed in figures 3 and 4.

**FIGURE 7** pH-dependent fusion properties of amphoteric II systems. Liposomes comprising the indicated amounts of the anionic lipid were produced from CHIM and CHEMS **(A)** or MoChol and CHEMS **(B)** and their pH-dependent lipid mixing was monitored by FRET. All mixtures of CHIM/CHEMS have amphoteric character and display pH dependent fusion. Mixtures of MoChol/CHEMS are also all amphoteric, but liposomes with high amounts of MoChol do not fuse, probably due to the larger volume of the MoChol head group.



**FIGURE 8** Phase diagrams for amphoter II systems. The phase behavior of CHIM:CHEMS **(A)** or MoChol:CHEMS **(B)** was calculated assuming the formation of an ion-free lipid salt and ion recruitment to the overage of charged lipids. Higher values for  $\kappa(\text{pH})$  reflect the existence of a stable lipid phase at acidic and neutral pH, whereas lower values correlate with the existence of a fusogenic phase at slightly acidic conditions. **(B)** The inhibition of fusion for mixtures comprising more than 50mol% of MoChol corresponds with high values of  $\kappa(\text{pH})$  in the phase diagram.

**FIGURE 9** pH-dependent fusion and phase diagram of an amphoter III system. Liposomes comprising the indicated amounts of the anionic lipid were produced from MoChol and DOPA **(A)** and their pH-dependent lipid mixing was monitored by FRET. Mixtures comprising between 33 and 50mol% of DOPA have amphoteric character and display pH dependent fusion. **(B)** phase diagram for MoChol:DOPA assuming a lipid salt formation and counterion recruitment.

Figure 1

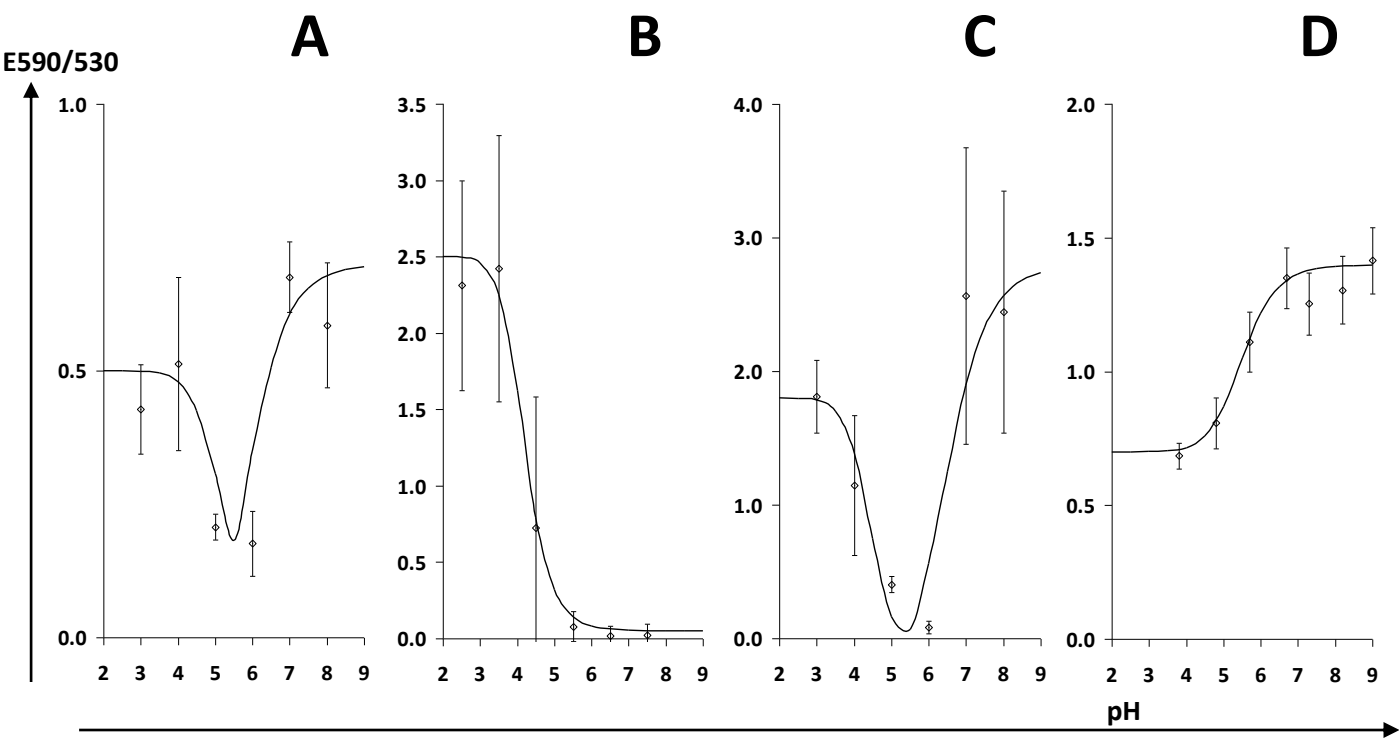


Figure 2

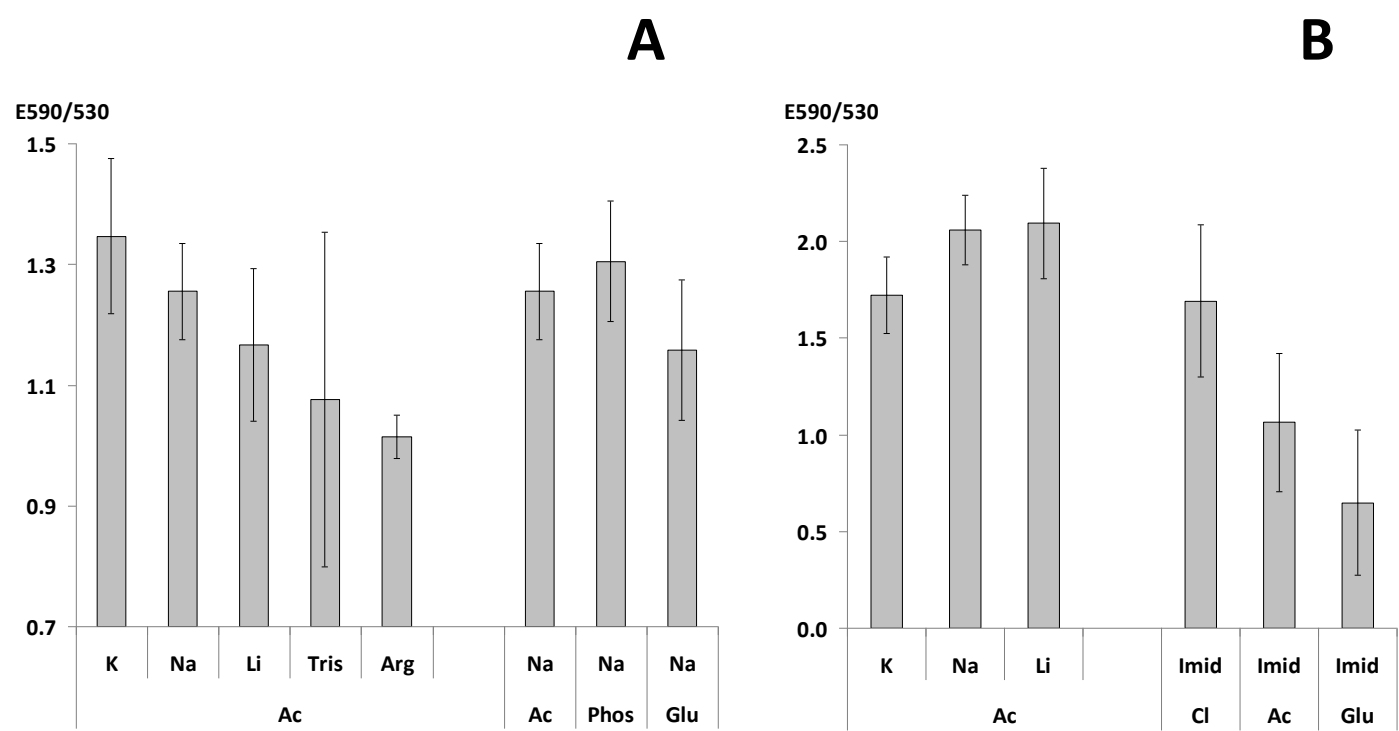


Figure 3

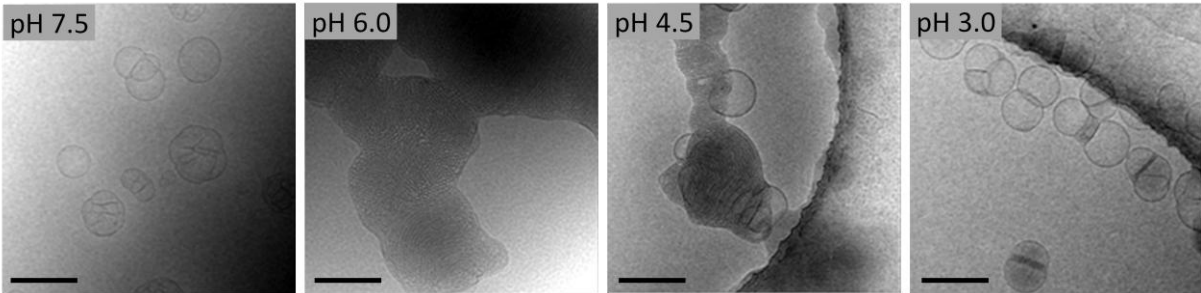


Figure 4

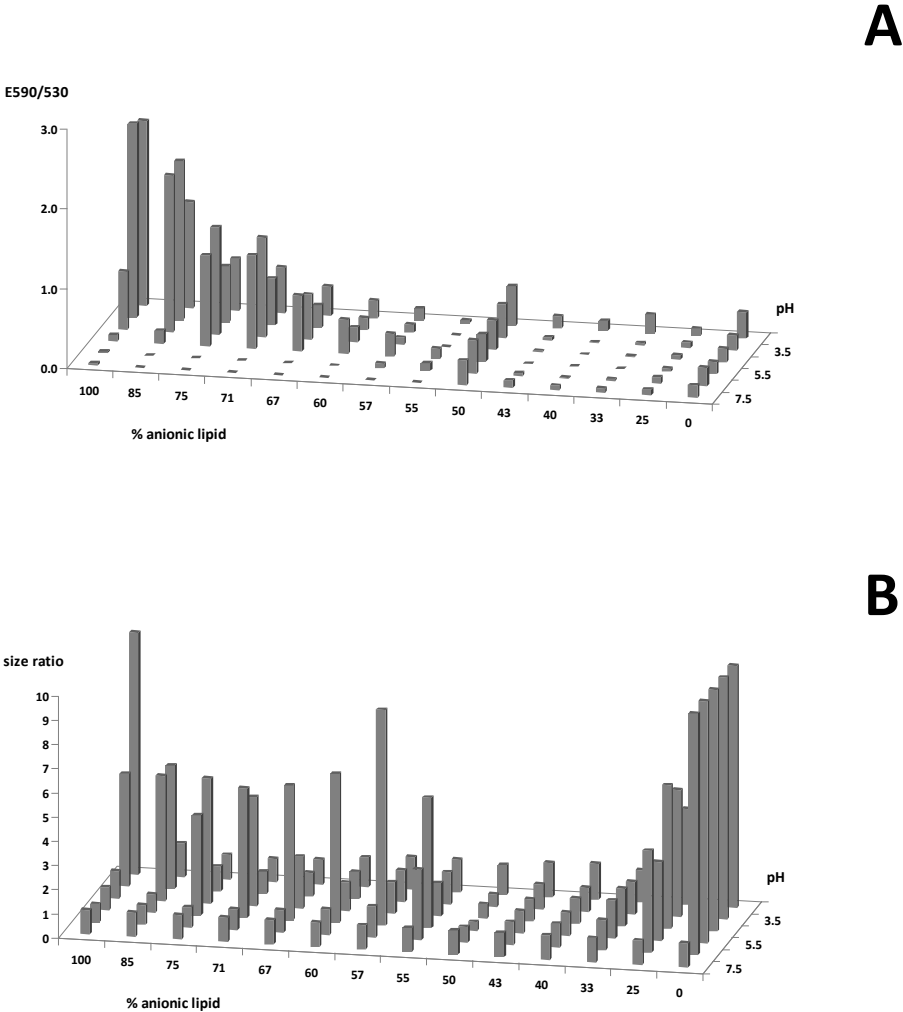


Figure 5

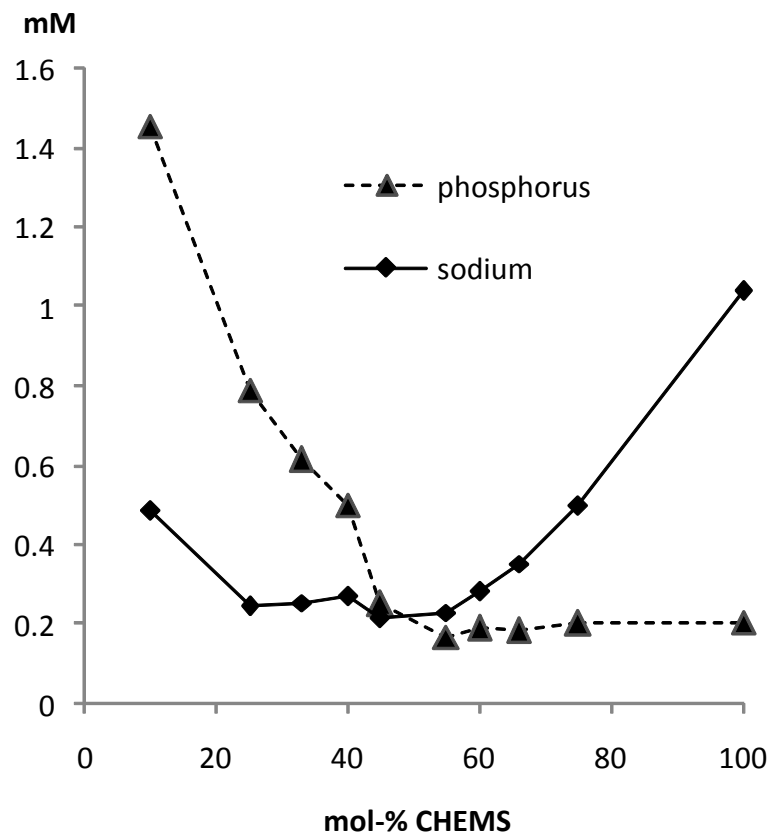
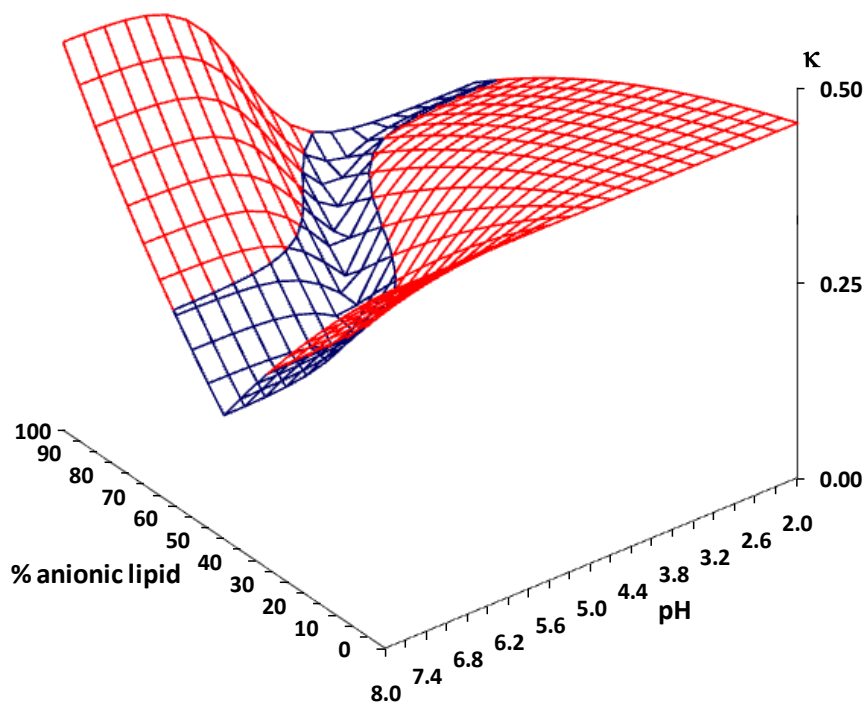
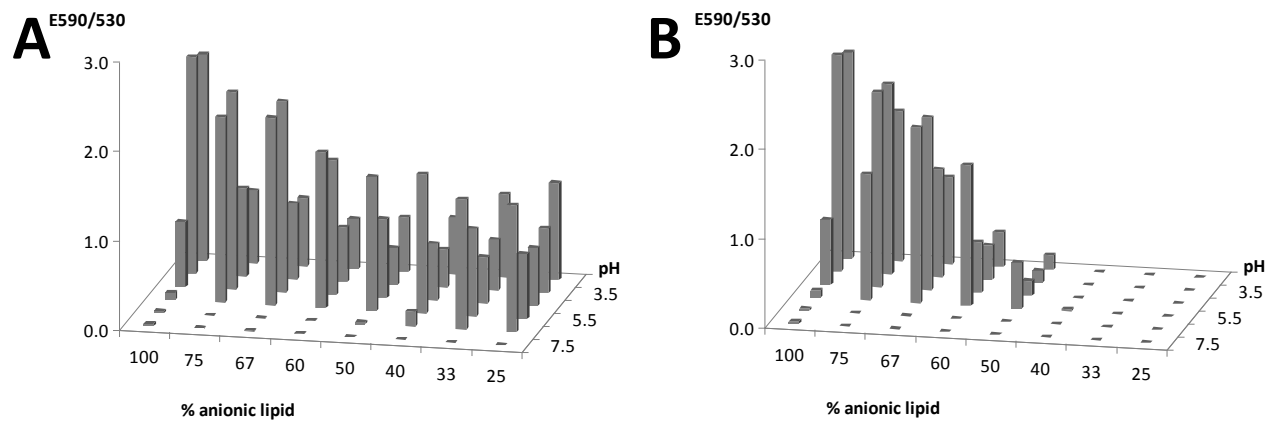


Figure 6



**Figure 7**



**Figure 8**

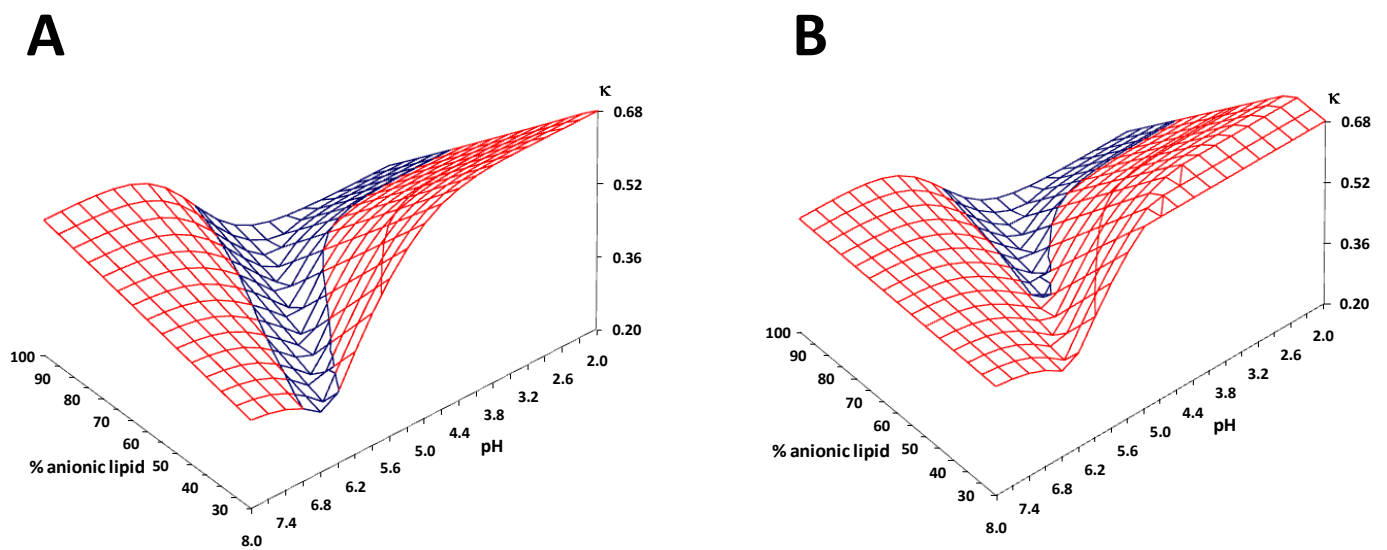
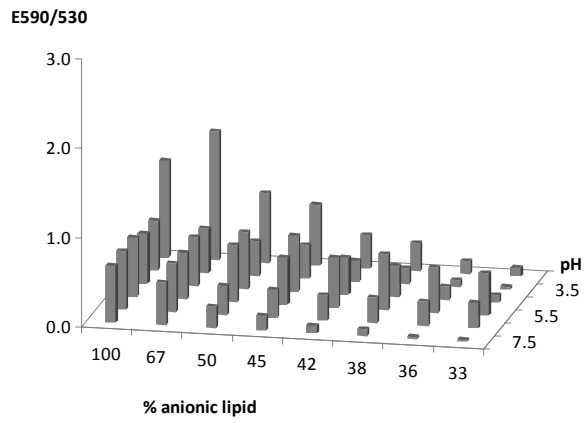


**Figure 9**

**A**



**B**

